MEDS Clinical Medicine (2023)
Clausius Scientific Press, Canada

DOI: 10.23977/medsc.2023.040213
ISSN 2616-1907 Vol. 4 Num. 2

Injection of New PMMA Loaded Microspheres into Anterior Chamber to Establish a Rabbit Glaucoma Model*

Shen Meitong[1,a], Koole Levinus Hendrik[2,b,*]

[1]School of Ophthalmology and Optometry (School of Biomedical Engineering), Wenzhou Medical University, Wenzhou, 325007, China
[2]Eye Hospital of Wenzhou Medical University, Wenzhou, 325007, China
[a]shenmeitong_eye@126.com, [b]1359992523@qq.com
[*]Corresponding author

Keywords: Glaucoma; PMMA*; Hydrogel; Glaucoma model; Anterior chamber injection

Abstract: Objective: To develop a novel PMMA material microsphere and characterize it. Named it PMMA*.The microsphere was loaded with drugs, and the intraocular pressure of rabbits was increased by anterior chamber injection, so as to establish a new animal model of ocular hypertension. Methods: PMMA* microspheres with a diameter of 50-80μm were prepared, and the drug loading, release and biosafety of PMMA* microspheres were analyzed. PMMA* microsphere suspension was prepared at 1% dosage of atropine sulfate. Eighteen healthy male New Zealand white rabbits were selected, with the right eye as the experimental eye and the left eye as the control eye. They were randomly divided into blank microsphere group, atropine sulfate group and atropine sulfate loaded microsphere group with 6 rabbits in each group. The chronic ocular hypertension model of the right eye was established. Intraocular pressure was monitored postoperatively and Micro-CT was used to determine the position of the microsphere at the anterior chamber Angle. The pathological changes of chronic glaucoma were studied. Results: PMMA* microspheres have the characteristics of micropore structure, adjustable size, slow release, in situ residence and good biosafety. There was no significant difference in preoperative intraocular pressure in rabbits ($P>0.05$), which was comparable. At 15 days after surgery, the intraocular pressure in experimental eyes was significantly higher than that in control eyes, with statistical significance ($P<0.05$), and the increase of intraocular pressure caused by drug-loaded PMMA* microspheres was more significant. Micro-CT determined the position of the microsphere in the anterior chamber Angle of rabbit. The atropine sulfate loaded microspheres showed more obvious ganglion cell - retinal nerve fiber layer damage. Conclusions:The PMMA* microspheres synthesized in this study have good drug loading performance and slow release performance. Intraventral injection of drug-loaded PMMA* microspheres can block the outflow of aqueous solution to establish a better chronic glaucoma model.

1. Introduction

Glaucoma is the second leading cause of blindness in the world[1], and there is a growing demand

for establishing reliable animal models for glaucoma research. Rabbit eyes are similar in size and aqueous humor outflow pathway to human eyes, which is a promising and convenient animal model for glaucoma research[2]. In this project, a novel polymer chemically synthesized microparticle (sphere) with unique microporous properties and in situ localization properties was explored. The chemical composition of the particles is similar to that of cross-linked polymethyl methacrylate (PMMA), but there are differences: (1) the particles contain a HEMA component that makes the particles partially hydrophilic (hydrogel), that is, water absorbent, and (2) the particles contain a 4-IEMA component that makes the particles opaque and can absorb x radiation. In this experiment, the biomaterial was named PMMA* microspheres. PMMA* microspheres can be used as drug delivery systems for controlled and sustained release of drugs at the corresponding parts of the organism. In rabbit eyes, the scleral venous plexus replaces the Schlemm canal[3], which is similar to human eyes and can simulate the outflow pathway of aqueous humor. Atropine can cause the elevation of intraocular pressure[4]. The rabbit model of chronic glaucoma was established by injecting PMMA* microspheres containing atropine sulfate into the anterior chamber to block the outflow pathway of aqueous humor. The drug loading effect of PMMA* microspheres was studied and the pathological changes of chronic glaucoma were studied.

2. Materials and Methods

2.1 General Information

Eighteen healthy New Zealand white rabbits, weighing 2.5-3kg, male, were purchased from Shanghai Weitong Lihua Company and raised in the animal room of the Experimental Animal Center of Wenzhou Medical University. Exclusion criteria: ①Abnormal anterior segment in slit-lamp examination; ②Fluorescein sodium staining score greater than 5; ③There was a significant difference in IOP between the two eyes of rabbits before operation ($P<0.05$), and there was no comparable rabbit. ④Rabbits with abnormal feeding and defecation. This study was approved by the Ethics committee of our university.

2.2 Methods

Then the morphology of the microspheres was observed by scanning electron microscope (SEM), the drug loading and release of the microspheres were measured by ultraviolet spectrophotometer (UV-Vis), and the biosafety of the microspheres was checked by cell experiment. The status of the purchased experimental animals was observed and the intraocular pressure was monitored before operation. The experimental animals were in good physical condition and the difference of intraocular pressure between both eyes was significant ($P<0.05$). Atropine sulfate loaded PMMA* microspheres suspension with 1% atropine sulfate solution was prepared for administration. The rabbit models of chronic glaucoma were established by injecting microsphere suspension into the anterior chamber of rabbits. The intraocular pressure was monitored and recorded 31 days after surgery. Zeiss high resolution optical coherence tomography (Cirrus-HD OCT) was used to measure the thickness changes of retinal layers in white rabbits. Micro-CT was taken to determine whether the microspheres could reside in situ in the anterior chamber Angle of the rabbit. Paraffin sections of rabbit eyes were stained with HE for observation of retinal tissue.

2.2.1 Synthesis of PMMA* microspheres

All synthesis steps were performed in a fume hood. First, a stock solution of synthetic microsphere solution was prepared by dissolving polyvinyl alcohol (64.0g), polyvinyl pyrrolidone (29.0g), and

polyethylene glycol (48.6g) in 2000 ml of water. Mechanical stirring was performed at room temperature until all polyvinyl alcohol was completely dissolved. This stock solution was stored at 4℃. Transfer the stock solution (400ml) to a 1L round-bottom flask. The flasks were heated by immersion in an oil bath placed on a magnetic stirrer connected to a temperature control system (contact thermometer). The contents of the flask were magnetically stirred (500 rpm) and heated to 90℃, followed by cooling to 50℃. The monomer mixture consisted of MMA (4.00g, 40.0mmol), HEMA (0.52g, 4.0mmol), EGDMA (3.96g, 20.0mmol), 4-IEMA (3.60g, 10.0mmol) and initiator (0.43g, 10.0mmol). 2.0mmol) were added to the stock solution through a polypropylene pipette and the temperature was again raised to 90℃. Ten minutes after reaching 90℃, a portion of the reaction mixture (about 1ml, glass pipette) was taken and mixed with about 10ml of cold water in a glass tube. The particles sank to the bottom of the tube. Microscopic examination revealed the presence of microspheres of different sizes. The temperature was maintained at 90℃ and stirring was continued for 60 minutes. "Then, turn off the heating, add cold water (200mL), and stop stirring when the mixture has cooled to room temperature." They were washed repeatedly with water (>6times), washed with 96% ethanol (1time), and washed again with water (3times). Clean pellets were collected in Petri dishes and dried overnight in an oven (37℃).

2.2.2 PMMA microspheres were photographed by scanning electron microscope

The 50-80μm, 80-100μm microspheres loaded with atropine and PMMA* microspheres without drug were evenly spread on the conductive glue attached to the sample stage of the scanning electron microscope, respectively. The gold was sprayed into the vacuum chamber of the ion sputter instrument, and the morphology and drug loading of the PMMA* microspheres were observed under the scanning electron microscope (SEM).

2.2.3 The drug loading and release of PMMA* microspheres were analyzed by ultraviolet spectrophotometer (UV-Vis)

Turn on the computer and preheat the spectrophotometer for 20 minutes before measuring the sample. After the quartz cuvette was cleaned, the reference line was corrected with the blank reagent, and then the sample to be tested was added for determination. After the measurements were completed, the tubes were cleaned for the next use.

①The standard curve of atropine sulfate determined by UV-vis spectrophotometer: turn on the machine and preheat for 30minutes. The baseline was calibrated by placing 2 cuvette with ultrapure water in the detection tank. 1% atropine solution was diluted into different concentrations of solution, UV-vis spectrophotometer (UV-vis) was set to zero, and the absorbance OD256 at 256nm was detected and recorded successively. The standard curve of atropine sulfate was obtained by plotting the linear curve of atropine sulfate solution concentration against OD256 using Graph Prism. The cuvette was removed, washed with ultrapure water to air dry, the computer and machine turned off, and placed in a drying bag in the test room. ②The release curve of atropine sulfate loaded microspheres in ultrapure water at different time points was determined by UV-vis spectrophotometer: 100mg of 50-80μm microspheres were soaked in 5% atropine solution for 24 hours, then the microspheres were removed, washed, and dried. Six reagent bottles were prepared, each containing 5mg atropine sulfate loaded with microspheres and immersed in 1ml ultrapure water. Calibration curves were obtained by placing 2 cuvette with ultrapure water in the detection tank. At 2h, 6h, 12h, 18h, and 24h after the start of immersion, the supernatants of each bottle were filtered and collected, and the absorbance at 256nm was measured and recorded. Using the atropine sulfate standard curve, the concentration of atropine sulfate solution corresponding to the absorption value was calculated. The release curves of atropine sulfate loaded microspheres in ultrapure water at different times were

plotted using Graph Prism. The cuvette was removed, washed with ultrapure water, and allowed to air dry. Turn off the computer and put it in a dry bag. ③The release of atropine sulfate loaded microspheres in ultrapure water after 12h was determined by UV-visible spectrophotometer: 100mg of 50-80μm microspheres were soaked in 5% atropine solution for 24h, then the microspheres were removed and washed and dried. Ten mg of pellets containing atropine sulfate were immersed in 2ml ultrapure water for 12 hours. Turn on the machine and warm up for 30 minutes. Two cuvette containing ultrapure water were placed in the detection tank to calibrate the baseline. The supernatant of the atropine sulfate pellet suspension was collected at 12h, and the absorbance was measured at 256nm and recorded. Using the atropine sulfate standard curve, the absorbance value corresponding to the concentration of atropine sulfate solution was calculated. The cuvette was removed, washed with ultrapure water to air dry, the computer and machine turned off, and placed in a drying bag in the test room.

2.2.4 Cell experiments

2.2.4.1 CCK-8 assay

In this experiment, CCK-8 kit was used to detect the effect of 300-500μm and 500-700μm PMMA microspheres on the survival rate of HCEC and L929 cells. Three groups were set up, namely control group, experimental group and blank group. Data processing: The apoptosis rate was calculated by (ODexperimental group -OD blank)/ (OD control group -OD blank) *100% formula. Prism software was used for data processing and chart making.

2.2.4.2 Cell death/viability staining (Calcein-AM/PI staining)

Live/dead cell staining is used to stain live and dead cells by Calcein-AM/PI double staining of cells [5]. The viability of HCEC and L929 cells was detected by live/dead cell staining after 300-500μm and 500-700V PMMA microspheres were prepared. They were divided into experimental group and control group.

2.2.5 Rabbits were injected into the anterior chamber

2.2.5.1 A suspension of PMMA microspheres with 1% atropine sulfate was configured for administration

1% atropine solution was diluted into different concentrations, and the absorption peak at 256nm was measured by UV-vis spectrophotometer (UV-VIS) to draw the standard concentration curve. A total of 100 mg of 50 to 80 mm microspheres were soaked in 5% atropine solution for 24 hours, removed, washed, and allowed to dry. Ten mg of pellets containing atropine sulfate were immersed in 2ml ultrapure water for 12h. The suspension of the microspheres was filtered through a filter membrane, and the UV absorption peak of the clear solution at 256nm was measured using a UV-vis spectrophotometer. After half dilution of the clear solution with ultrapure water, the absorption peak at 256nm was 2.9987. This value is similar to the absorption peak at 256nm in a solution of 1% atropine diluted in half. A suspension of microspheres was prepared from 10 mg of PMMA* microspheres with a particle size of 50 to 80um with 2ml ultrapure water.

2.2.5.2 Rabbits were injected into the anterior chamber

Eighteen healthy male New Zealand white rabbits weighing 2.5-3kg were randomly divided into 3 groups with 6 rabbits in each group: blank microspheres group, atropine sulfate group, and atropine sulfate loaded microspheres group. The anterior segment of the rabbits was normal by slit lamp

examination and the fluorescein sodium staining score was less than 5. Anesthesia was considered moderate when the corneal reflex disappeared, the muscles of the limbs and abdomen were relaxed, and the breathing was stable. The right eye of each rabbit was used as the experimental eye and the left eye as the control eye. After routine disinfection, the towel was spread, the surgical instruments were disinfected, the eyelid opener was placed, and the conjunctival sac was rinsed with diluted iodophor solution. In the blank microspheres group, the right eye was injected with blank microspheres suspension 0.2ml (5mg/ml), and the left eye was injected with normal saline 0.2ml. In the atropine sulfate group, the right eye was injected with 1% atropine sulfate solution 0.2ml, and the left eye was injected with normal saline 0.2ml. In atropine sulfate loaded microspheres group, the right eye was injected with 1% atropine sulfate microspheres suspension (0.2ml, 5mg/ml), and the left eye was injected with normal saline (0.2ml). The results of surgery are shown in Figure 1.

Figure 1: Anterior injection under the operating microscope

2.2.6 Intraocular pressure measurement

Icare TONOVET Plus tonometer was used to measure the intraocular pressure of rabbits at the same time each day while they were awake, 1-3 days before modeling and every two days after surgery. Holding the tonometer in the right hand, the tip of the measuring needle was perpendicular to the middle area of the antenna membrane, and the results of intraocular pressure were measured and recorded (confidence interval≧95%), and the measured value under the agitation of the white rabbit or the artificial factors were removed. Six effective IOP values were recorded for each eye, and the average value was used as the IOP value.

2.2.7 The thickness of each retinal layer in rabbit eyes was measured by OCT

The retinal ganglion cell-inner plexiform layer (Rplexiform layer) was measured by Cirrus-HD OCT in experimental and control rabbits. GCIPL) and GCL thickness [6], and the differences in thickness changes between the experimental eyes of each group were evaluated.

2.2.8 Micro-computed Tomography (Micro-CT)

Micro-CT is a micro-focus X-ray tube different from ordinary clinical CT, which can be used to scan and analyze living small animals or a variety of hard tissues and related soft tissues [7]. The experimental methods are as follows:

After 1 month of continuous observation, the rabbits were killed by air embolization, the eyeballs were completely removed, and the optic nerve of 1 to 3mm was retained. The eyeballs were immersed in paraformaldehyde fixative and placed in a refrigerator at 4℃ overnight. The rabbit eye was placed in the EP tube, the EP tube with the rabbit eye was placed on the Micro-CT operating table, and the machine was started to set the parameters (X-ray voltage was 65kV, current was 380uA) for observation.

2.2.9 Methods of sampling and pathological section preparation

After 31 days of intraocular pressure measurement, the rabbits were killed by air embolism, and the rabbit eyeballs were completely harvested and the 1mm-2mm optic nerve was retained.The retinal tissue of the white rabbit was subjected to paraffin section and hematoxylin-eosin (HE) staining. Observations were made under a light microscope and recorded.

2.2.10 Immunofluorescence staining technique

The rabbits were euthanized by injecting air into the ear vein and enucleation of the eyeball was performed immediately after the treatment. Eyeballs were embedded in paraffin, and paraffin sections (3μm) of rabbit eyes were made along the eye axis, deparaffinized and hydrated. After several rinses in phosphate buffered saline (PBS), sections were made. Incubation was performed overnight at 4◦C with the following primary antibodies: rabbit anti-mouse glial acidic fibrin (GFAP) (DAKO, Glostrup, Denmark) at a 1:1000 dilution; Rabbit anti-rat glutamine synthetase (GS) (Sigma-Aldrich, St Louis, MO, USA)1:500 dilution; Goat anti-human Iba1 (Abcam, Cambridge, UK) diluted 1:100; Mouse anti-mouse PKCα (Sigma-Aldrich) was diluted 1:100; Goat anti-mouse (Santa Cruz Biotechnology, Heidelberg, Germany) was diluted 1:100. After washing with PBS, rabbit anti-goat Alexa 568 was incubated twice with goat anti-rabbit 568 solution and rabbit anti-mouse 568 solution for 2 h at room temperature (Invitrogen, Carlsbad, CA, USA) antibody. SYTOX Green nucleic acid staining (Invitrogen) was diluted in PBS (1:500 dilution) and incubated for 10 min for nuclear counterstaining. Slides were mounted on fluorine slides (Sigma-Aldrich) medium for further analysis using a laser scanning confocal microscope (TCS SP5; Leica Microsystems GMBH, Heidelberg, Germany).

2.3 Statistical methods

SPSS 25.0 was used for statistical analysis, measurement data were expressed as mean ±SD, and Mann Whitney U test was used for comparison between the two groups. Categorical variables were analyzed by univariate and multivariate Logistic regression analysis. $P<0.05$ was considered statistically significant.

2.4 Results

2.4.1 The results were measured by ultraviolet spectrophotometer (UV-Vis)

(1) Atropine sulfate standard curve: the maximum absorption peak of atropine sulfate solution was found at 256nm by full spectrum scanning. The absorbance of different concentrations of atropine sulfate solution was measured, and the relationship between concentration and absorbance curve was drawn. As shown in FIG. Ii, the absorbance of atropine sulfate was linearly dependent on the concentration. (y=609.5x+0.06720, x: concentration of atropine sulfate solution, y: absorption peak at 256nm). See Figure 2.

(2) Release curve of atropine sulfate drug-loaded microspheres: 6 reagent bottles were loaded with 5mg atropine sulfate loaded microspheres in 1ml ultrapure water. After immersion for 2h, 6h, 12h, 18h, and 24h, the supernatant of each bottle was collected after filtering off the microspheres, and its absorbance was measured at 256nm. The above was repeated three times to produce the figure shown in Figure 3.

(3) Drug loading analysis of atropine sulfate microspheres:

The data in Figures 2 and 3 allowed us to calculate the drug loading on the atropine loaded microspheres. Assuming that atropine was completely dissolved after 12 h (see Figure 3), the concentration of the supernatant could be calculated from the absorption peak (OD256): the

experimental value of OD256 was 2.9, and the concentration = 0.0046 mg/mL = 4.6 g/mL can be obtained from the equation in Figure 2. Since the release experiments were performed in 2.0 mL of supernatant, this means that 2* 4.6 = 9.2g of atropine sulfate was released from 5.0 mg microspheres. Thus, the atropine sulfate loading of the microspheres was (9.2/5000)* 100% = 0.2%

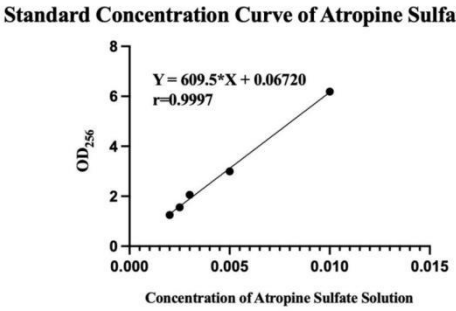

Figure 2: Absorbance standard curve of atropine sulfate solution at 256nm

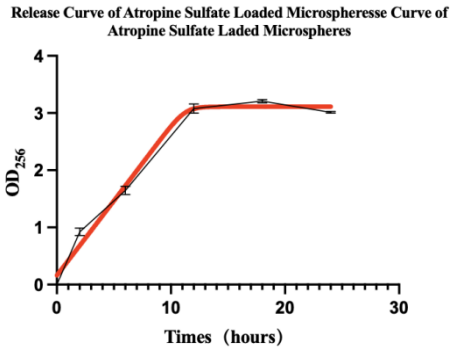

Figure 3: Release curve of atropine sulfate loaded microspheres in ultrapure water

The drug-loaded microspheres suspension was injected into the anterior chamber as described above. 8 mg atropine equivalent to the anterior chamber was introduced into the anterior chamber. "Typically, a 0.1% atropine solution is used clinically, so each eye drop (average volume 30 mL= 30 mg = 30000mg) contains 30 mg atropine." It is well known that 90% of each eye drop is lost in the first few seconds after instillation due to blinks and the limited size of the lacrimal sac in the eye. So, this leaves 3 mg of atropine sulfate to be absorbed by the eye. Apparently, only a small fraction of this 3 mg atropine sulfate reaches the anterior chamber. It follows that approximately 8 mg of atropine sulfate was injected into the anterior chamber with the loaded microspheres, much more than the amount of atropine sulfate that could reach the anterior chamber during eye drop treatment.

2.4.2 Results of SEM characterization of PMMA* microspheres

Different sizes of microspheres (50-80μm, 80-100μm) were screened by an oscillator. Scanning electron microscopy (SEM) was used to characterize the morphology and drug loading of drug-loaded and drug-free PMMA* microspheres. Most PMMA* microspheres are single uniformly dispersed particles of uniform size. Drug loading was visible on the surface of loaded PMMA* microspheres. See Figure 4.

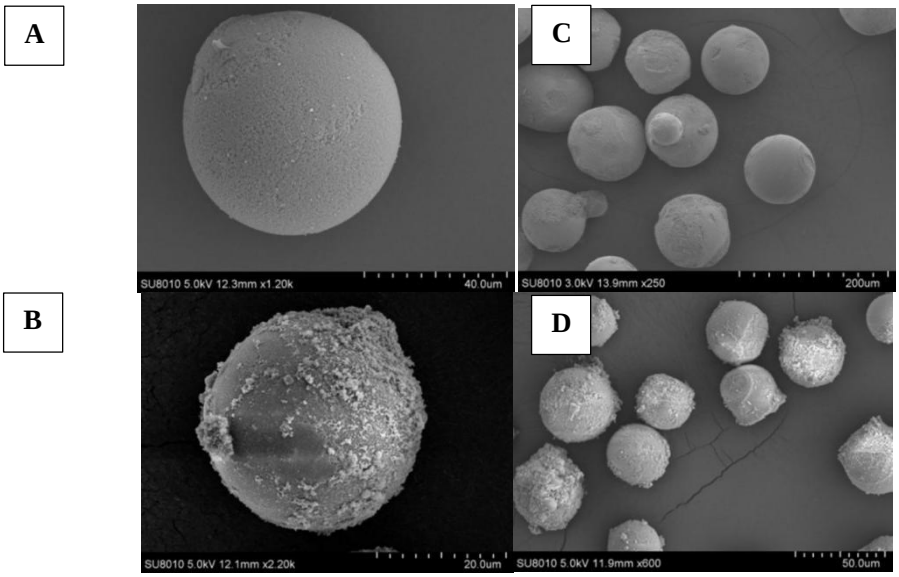

Figure 4: Observation of microspheres under scanning electron microscope (A: scale bar of PMMA microspheres without drug loading 40 μm; B: Atropine sulfate loaded PMMA microspheres, 20μm; C: scale bar of PMMA microspheres without drug loading 200 μm; D: scale bar of atropine sulfate loaded PMMA microspheres 5μm).

2.4.3 The biocompatibility of the PMMA microspheres to HCECs and L929 cells was observed by ordinary optical microscope

Equal amounts of 50-80 μm and 80-100 μm microspheres were co-cultured with HCECs and L929 cells for 24 hours, respectively, and were observed and photographed under a light microscope. The results are shown in Figure 5.

Microsphere-cell co-culture was observed under ordinary light microscope

Control	50-80μm	80-100μm

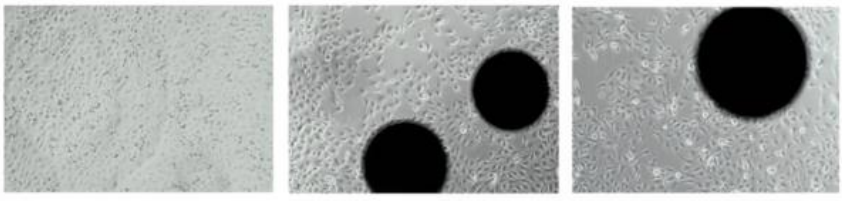

(a) HCECs

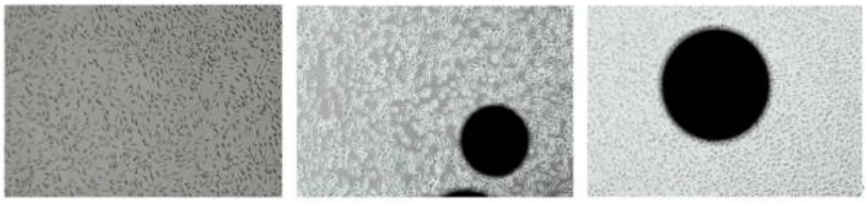

(b) L929

Figure 5: Ordinary light microscope images of blank microspheres co-cultured with (a) HCECs, (b) L929 for 24h

2.4.4 CCK-8 results

It is necessary to evaluate the cytocompatibility of PMMA* microspheres before using them in an

in vivo glaucoma model. CCK-8 results showed (Table 1, Figure 6) that compared with the control group, the cell viability of HCECs and L929 cells co-cultured with the microspheres for 24h was above 78%, which was statistically significant compared with the control group ($P<0.05$), indicating that the PMMA* microspheres had good biocompatibility for HCECs and L929 cells.

Table 1: Effect of different sizes of microspheres on the viability of HCECs and L929s cells (Note: n=6, $\bar{x} \pm s$, * compared with control group, $P<0.001$)

	HCECs	L929s
Control	100 ±0.000*	100 ±0.000*
50-80 μm	81.68 ±0.013*	82.86 ±0.002*
80-100 μm	85.37 ±0.014*	89.15 ±0.005*

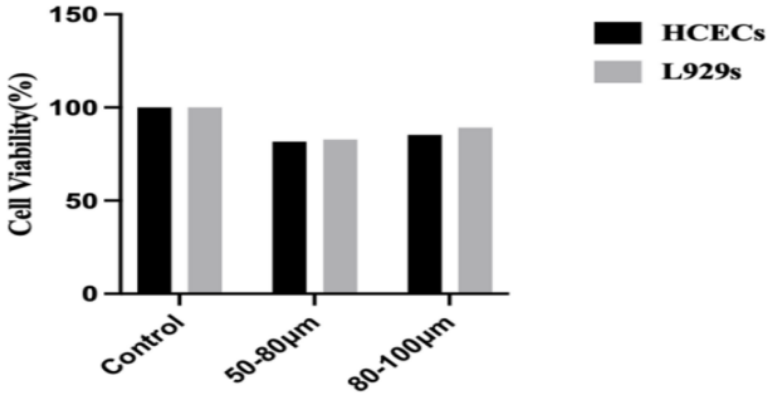

Figure 6: Determination of the viability of HCECs cells and L929 cells after 24h of co-incubation with blank microspheres

2.4.5 Results of cell death/viability staining assay

Based on CCK-8 results, HCECs and L929 cells were stained with Calcein-AM and propidium iodide (PI). Under the fluorescence microscope, live cells appear green and dead cells appear red. The images showed (Figure 7) that after 24 hours of co-culture of different sizes of PMMA* microspheres with HCECs and L929 cells, most of the HCECs and L929 cells in each group were living green cells with good growth condition and few dead red blood cells. See Figure 7.

Results of live and dead staining of HCECs

Control	50-80μm	80-100μm

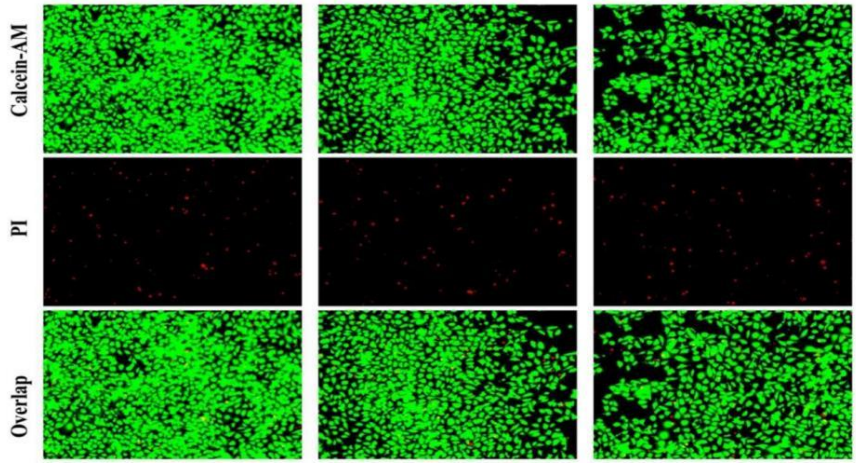

Results of live and dead staining of HCECs

Control	50-80μm	80-100μm

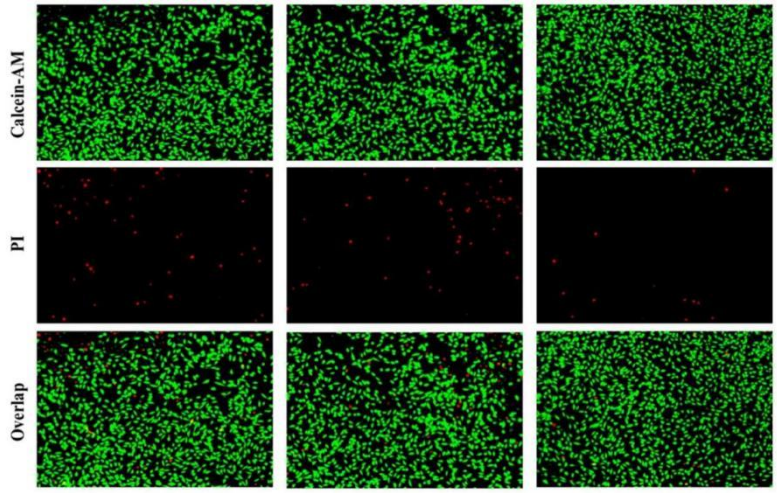

Figure 7: Growth status of HCECs and L929 observed by cell death/viability staining

2.4.6 Preoperative intraocular pressure

Paired sample t test showed that the average intraocular pressure of the experimental eyes in the atropine sulfate loaded microspheres group was 18.33±0.47mmHg. The average intraocular pressure in the control group was 18.11±0.34mmHg. The average intraocular pressure of rabbits in atropine sulfate group was 18.5±0.36mmHg. The average intraocular pressure in the control group was 18.83±0.28mmHg. The mean intraocular pressure of the blank microspheres group was 18.05±0.47mmHg. The mean IOP of the control group was 17.89±0.24mmHg. There was a significant difference in IOP among the three groups (p=0.01) (Figure. 8).

	Atropine sulfate + microspheres group			Atropine sulfate group			Blank microspheres group		
	Control Eyes	Experimental Eyes	P	Control Eyes	Experimental Eyes	P	Control Eyes	Experimental Eyes	P
-1d	18.50±0.50	18.33±0.63	0.013	19.83±0.27	19.17±0.25	0.005	17.67±0.33	17.00±0.50	0.003
-2d	18.17±0.20	18.00±0.57	0.005	18.17±0.33	18.00±0.50	0.016	18.83±0.13	18.83±0.25	0.013
-3d	17.67±0.33	18.67±0.20	0.003	18.50±0.25	18.33±0.33	0.005	17.17±0.25	18.33±0.67	0.004

Figure 8: IOP values in each group three days before surgery

2.4.7 Postoperative intraocular pressure

The IOP of some rabbits was maintained above 20mmHg at 4 weeks after operation. A few may be maintained for 6-9 weeks. There was a significant difference in nocturnal intraocular pressure between the experimental group and the control group from day 1 to day 27 after injection ($p<0.05$), but there was no significant difference in nocturnal intraocular pressure between the experimental group and the control group 28 days after injection ($p<0.05$). There were statistically significant differences in the daytime intraocular pressure between the experimental group and the control group on the 6th, 7th, 8th, 9th, 10th, 12th, 14th, 16th and 19th days after surgery ($p<0.05$). GraphPad Prism software was used to produce images (see Figure 9).

	Atropine sulfate +microspheres group			Atropine sulfate group			Blank microspheres group		
	control eyes	experimental eyes	P	control eyes	experimental eyes	P	control eyes	experimental eyes	P
1d	15.33±0.67	14.83±0.85	0.003	17.17±0.56	16.83±0.25	0.019	15.67±0.25	15.00±0.33	0.026
3d	15.67±0.33	15.00±0.55	0.014	16.00±0.78	17.17±0.75	0.003	15.83±0.50	16.83±0.50	0.015
5d	14.33±0.12	16.83±0.67	0.034	17.33±0.12	18.50±0.38	0.014	16.17±0.33	16.33±0.67	0.036
7d	16.17±0.33	18.83±0.12	0.028	18.33±0.15	19.63±0.83	0.009	16.67±0.50	17.00±0.12	0.035
9d	15.00±0.50	19.83±0.87	0.027	18.67±0.33	20.00±00.19	0.017	15.17±0.33	17.67±0.35	0.018
11d	16.67±0.33	19.67±0.67	0.018	18.00±0.25	19.00±0.25	0.023	16.79±0.36	17.67±0.50	0.013
13d	18.17±0.67	20.33±0.45	0.019	18.33±0.10	19.00±0.33	0.025	17.00±0.25	18.33±0.33	0.042
15d	19.00±0.50	21.00±0.75	0.011	19.00±0.67	20.25±0.15	0.016	17.67±0.75	19.00±0.12	0.092
17d	19.00±0.33	21.67±0.35	0.039	18.17±0.38	20.17±0.89	0.035	18.13±0.25	20.33±0.50	0.006
19d	19.00±0.67	22.00±0.24	0.021	18.67±0.33	19.33±0.75	0.019	18.33±0.90	20.67±0.15	0.018
21d	19.50±0.20	23.13±0.87	0.062	19.00±0.33	18.33±0.13	0.013	17.67±0.57	20.33±0.50	0.038
23d	18.83±0.82	23.67±0.29	0.019	18.33±0.12	18.00±0.95	0.047	18.00±0.56	21.25±0.85	0.014
25d	18.17±0.39	24.50±0.67	0.006	18.67±0.56	18.00±0.25	0.041	18.50±0.45	22.67±0.36	0.082
27d	18.00±0.50	25.17±0.29	0.017	19.00±0.50	19.13±0.33	0.083	18.33±0.50	22.50±0.42	0.019
29d	18.83±0.67	27.83±0.19	0.041	19.00±0.25	19.00±0.73	0.016	19.00±0.33	23.00±0.50	0.061
31d	19.17±0.25	28.00±0.37	0.028	18.67±0.25	18.87±0.25	0.036	18.67±0.50	23.50±0.25	0.049

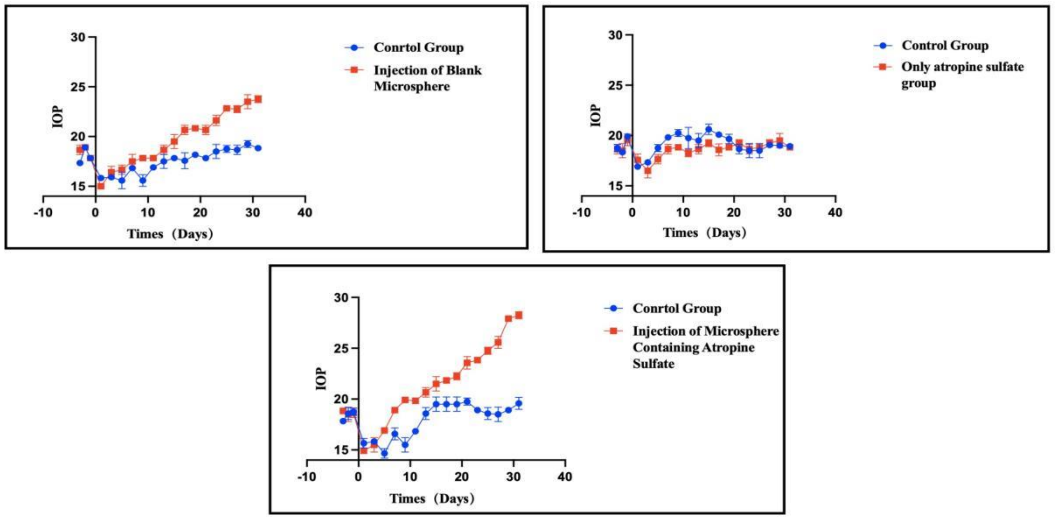

Figure 9: Comparison of IOP elevation between experimental eyes and control eyes in each group of white rabbits

2.4.8 Comparison of retinal thickness

The thickness of GCIPL and retinal fiber layer (RNFL) was measured by OCT in all rabbits 31 days after surgery (Table 2, Table 3, Figure 10).

Table 2: Thickness of GCIPL in experimental and control eyes of white rabbits in each group

	Control eye μm)	Experimental eye (μm)	p
Blank microspheres group	74.38±7.27	58.41±8.29	<0.05
Atropine sulfate group	78.64±6.87	79.76±4.86	<0.01
Atropine microspheres group	79.39±5.38	50.74±3.91	<0.05

Table 3: RNFL thickness in experimental and control eyes of white rabbits in each group

	Control eye (μm)	Experimental eye (μm)	p
Blank microspheres group	92.59±10.21	74.62±11.65	<0.05
Atropine sulfate group	96.39±8.93	95.43±9.85	<0.05
Atropine microspheres group	98.72±4.76	69.84±8.61	<0.05

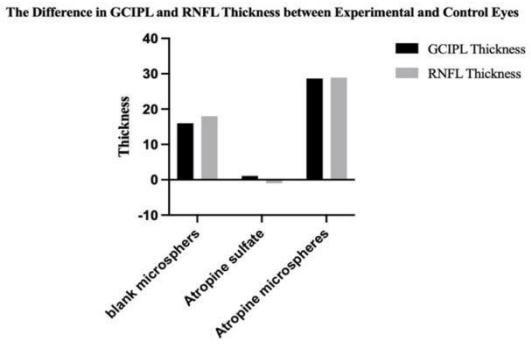

Figure 10: Comparison of measurement values of GCIPL and RNFL thickness parameters between the control group and the experimental group

2.4.9 Micro-CT was used to observe the inflow of microspheres into the anterior chamber Angle

As shown in Figure 11, most of the aqueous humor flow of the microspheres was blocked in the anterior chamber Angle of the rabbit eye compared to the normal rabbit eye, thus blocking the outflow path of the aqueous humor.

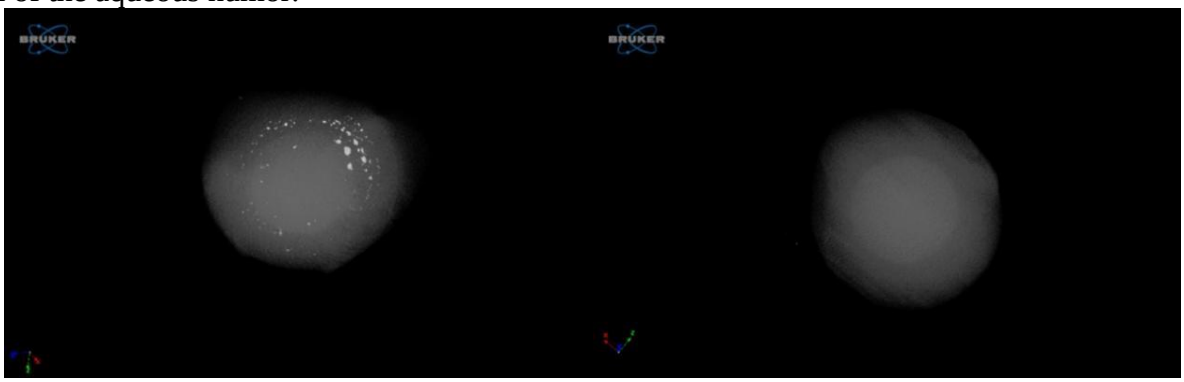

A B

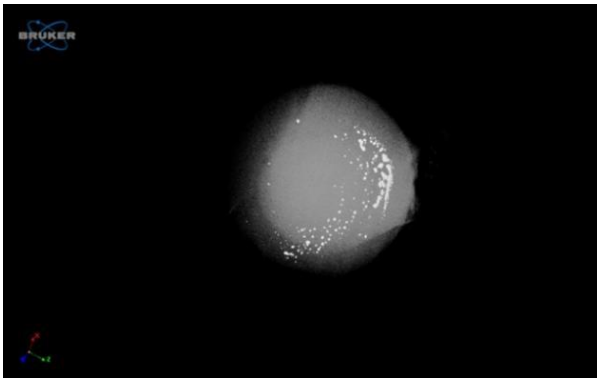

C

Figure 11: Micro-CT image of rabbit eye (A: Rabbit anterior chamber injected with blank microspheres; B: Rabbit eyes of control group; C: Rabbit anterior chamber injection of atropine sulfate microspheres)

2.4.10 Hematoxylin-eosin (HE) staining was used to observe the pathological changes of retina

HE staining showed that the retinal structure of normal rabbit eyes was clear and the cells in each layer were closely arranged. After 31 days, compared with the control group, the retinal thickness of

blank microspheres group and atropine sulfate loaded microspheres group showed varying degrees of reduction, ganglion vacuolization and nerve fiber layer atrophy. Compared with the control group, the inner retinal ganglion cell layer and inner accessory layer of the atropine injected microspheres were thinner, and the retinal ganglion cells were sparsely and disorderly arranged (Figure 12).

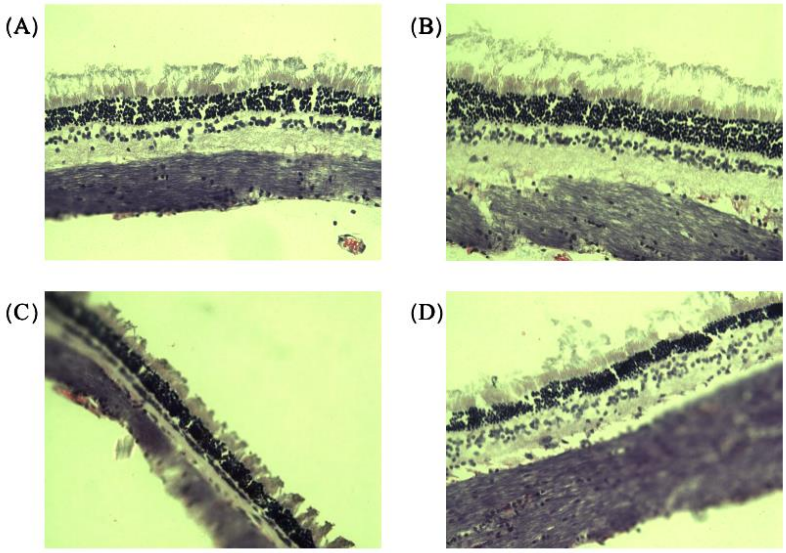

Figure 12: (A) representative images of HE staining of normal rabbit retina in the control group (×500); (B) representative images of HE staining of rabbit retina tissues injected with atropine sulfate only (×500); (C) representative HE staining images of rabbit retina tissues injected with atropine sulfate loaded microspheres (×500); (D) Representative images of HE staining of rabbit retinal tissue injected with blank microspheres (×500).

2.4.11 Hematoxylin-eosin (HE) staining was used to observe the pathological changes of anterior chamber Angle

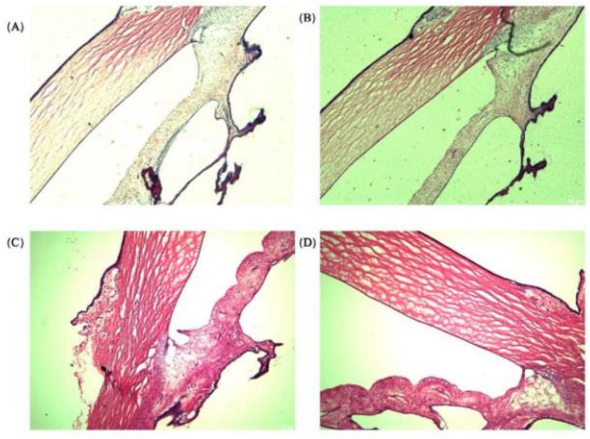

Figure 13: (A) Representative HE staining of the anterior chamber Angle of normal rabbits in the control group (×500); (B) representative HE staining image of the anterior chamber Angle of rabbits injected with atropine sulfate alone (×500); (C) Representative HE staining image of the anterior chamber Angle of rabbits injected with atropine loaded microspheres (×500); (D) Representative images of HE staining of the anterior chamber Angle of rabbits injected with blank microspheres (×500).

Thirty-one days after chronic ocular hypertension, HE staining of the anterior chamber Angle

showed that the anterior chamber of the normal rabbit eyes in the control group (A) was moved forward, the ciliary body was broken, and connected with the iris. The morphology of the anterior chamber of rabbits injected with atropine sulfate (B) was similar to that of the anterior chamber of control rabbits (A). Blank microspheres (C) and atropine sulfate microspheres (D) were used to induce chronic ocular hypertension for 1 month. The microsphere blocked the anterior chamber Angle, and the pathological section of the chamber Angle showed that the chamber Angle was round and blunt, and the ciliary blood vessels were filled with red blood cells, some of which adhered to the corneal endothelium. Figure 13.

2.4.12 Results of immunofluorescence staining

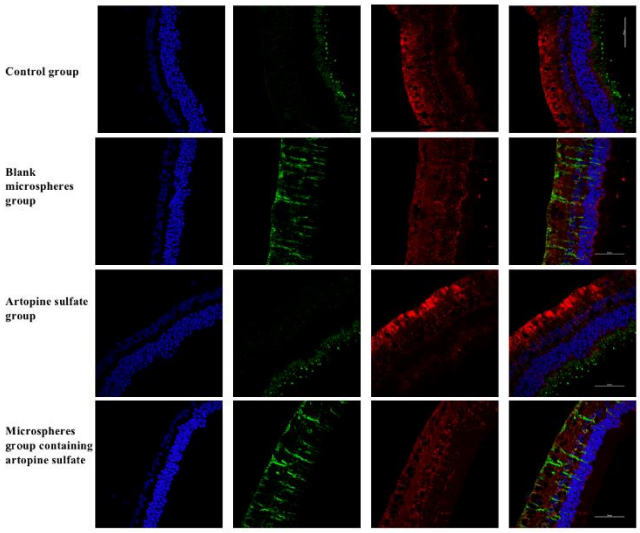

Figure 14: Expression of glial fibrillary acidic protein (GFAP) (green fluorescence) in each group. The expression of GAFP in Muller cells of blank microspheres group and atropine sulfate loaded microspheres group was observed by red fluorescence.

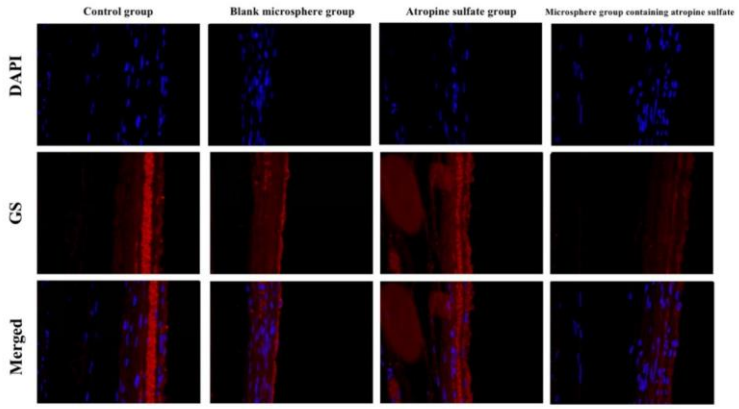

Figure 15: GS immunofluorescence pattern (×600) of Muller cells in rabbit retina 31 days after establishment of chronic ocular hypertension model.

Eighteen models of postoperative chronic ocular hypertension were analyzed by immunofluorescence technique. Anti-GFAP was used to label astrocytes and Anti-GS was used to label Muller cells [9]. In normal control rabbit eyes, astrocytes were restricted to the retinal ganglion cell layer. Anterior chamber injection of blank microspheres and atropine sulfate microspheres caused chronic ocular hypertension, and GFAP expression was observed in Muller cell gliosis in patients

with chronic ocular hypertension, see Figure 14.

Glutamine synthetase (GS) is the main enzyme involved in glutamate metabolism in Muller cells. It catalyzes the conversion of glutamate to glutamine, which is an essential component of glutamate recycling between neurons and glial cells. Because excessive extracellular glutamate is toxic to neurons and uptake of excessive extracellular glutamate by Muller cells can aggravate glaucomatous retinal cell loss, glutamine synthetase (GS) expression is reduced in Muller cells of eyes with high IOP (Figure 15). Immunofluorescence and intensity analysis showed that GS expression was higher in Muller cells in the control group than in the other three groups. Among them, only the atropine sulfate injection group had the strongest expression of GS in Muller cells, and the microspheres loaded with atropine sulfate injection group had the weakest expression of GS.

3. Discussion

At present, glaucoma is the second leading cause of blindness in the world. In recent years, the incidence of glaucoma has been increasing, and the research on glaucoma has become a research hotspot in ophthalmology [10]. There are no obvious symptoms in the early stage of chronic glaucoma, but eye distension, headache, blurred vision, optic nerve and visual field damage occur in the late stage of chronic glaucoma [11]. Therefore, the study of glaucoma has become imperative, and it is urgent to establish a simple, low-cost, long-lasting and stable glaucoma animal model with high intraocular pressure.

In this study, we first fabricated PMMA* microspheres. Throughout the preparation process, we can control the pore size and size of the hydrogel particles by controlling the proportion of reactants and the reaction conditions as well as the rate of reactant addition. The microspheres have a microporous structure and adjustable size, which enables large-scale preparation and synthesis of hydrogel materials. Since accurate material characterization is an essential step to ensure its successful synthesis and determine its application properties, we confirmed the successful preparation of the synthesized PMMA* microspheres by scanning electron microscopy (SEM) and UV-vis spectroscopy (UV-vis) and found that the synthesized PMMA* microspheres had good drug loading capacity. Good biocompatibility is considered to be one of the most important characteristics of biomaterials in biomedical applications such as bioimaging, biosensing, drug delivery, and disease therapy. Studies have shown that PMMA biomaterials have low cytotoxicity and good biocompatibility. In this study, CCK-8 and live/dead cell staining were used to determine the cytotoxicity. The study confirmed that PMMA microspheres had no obvious cytotoxicity after co-culture with HCECs and L929 cells for 24h, which was consistent with the low cytotoxicity of PMMA* materials reported in a previous study[12].

Current studies have shown that elevated IOP is usually due to a decrease in two aqueous humor channels through the anterior segment, the conventional channel and the uveoscleral outflow channel [13]. At present, the methods for establishing animal models of chronic glaucoma can be divided into destroying the structure of trabecular meshwork, increasing the scleral venous pressure, blocking the outflow channel of aqueous humor, and transgenic spontaneous ocular hypertension models according to their mechanisms [14]. Based on the important role of aqueous humor outflow pathway, Schlemm canal and uveal-scleral outflow pathway in the process of aqueous humor outflow, we used PMMA* microspheres of appropriate size to block the aqueous humor outflow pathway to establish a rabbit model of ocular hypertension. The intraocular pressure was increased by increasing the resistance of aqueous humor outflow to simulate the pathogenesis of glaucoma. In addition, atropine sulfate is a typical drug that blocks M choline receptors. M-choline receptor blockers have the effects of anti-M choline, relieving spasm of gastrointestinal smooth muscle, inhibiting secretion of glands, dilated pupils, increasing intraocular pressure, accelerating heart rate, and bronchiectasis. Atropine

has no effect on normal intraocular pressure, but in patients with abnormal intraocular pressure or narrow anterior chamber Angle or shallow anterior chamber, atropine sulfate can cause dilated pupils and Angle obstruction, which can significantly increase intraocular pressure and induce the risk of acute glaucoma. Studies have shown that the use of atropine can induce acute angle-closure glaucoma [15]. Due to the excellent drug-loading performance of PMMA* microspheres, atropine sulfate loaded on PMMA microspheres and slowly released into the anterior chamber of rabbits at 1% atropine sulfate administration concentration can cause a sharp increase in intraocular pressure in rabbit eyes and maintain high intraocular pressure for at least one month, so as to establish a good animal model of ocular hypertension glaucoma.

In the present study, this model was successfully established in New Zealand white rabbits. In the rabbit anterior chamber injection group, the intraocular pressure of the experimental eyes injected with atropine sulfate did not increase significantly compared with the control eyes injected with the same amount of normal saline during the whole observation period of 31 days, and the change of the intraocular pressure of the experimental eyes was relatively stable with small fluctuations. In the rabbit eyes injected with blank PMMA microspheres, the intraocular pressure of the experimental eyes injected with blank PMMA microspheres was higher than that of the control eyes injected with the same amount of normal saline during the whole observation period of 31 days. In the experimental group of 6 rabbits, the average intraocular pressure increased on the 15th day after operation. The intraocular pressure increased to (23.5±0.25) mm Hg on the 31st day after operation, which was about 5mmHg higher than that of the contralateral eye. From the 15th to 31st day after operation, the intraocular pressure of the rabbit eyes continued to increase compared with the control group, maintaining the state of high intraocular pressure glaucoma. In the group of rabbits injected with atropine sulfate loaded PMMA* microspheres in the anterior chamber, the intraocular pressure of experimental eyes injected with atropine sulfate was significantly higher than that of control eyes injected with the same amount of normal saline during the whole observation period, and the intraocular pressure of experimental eyes showed an upward trend 7 days after operation. The intraocular pressure increased to (28.00±0.37) mmHg on the 31st day after operation, which was about 10mmHg higher than that of the contralateral eye. In conclusion, when microspheres loaded with atropine sulfate were injected into the anterior chamber of rabbits, the combined effect of drug and microspheres would produce a more obvious upward trend of intraocular pressure.

Micro-CT images of rabbit eyes with high intraocular pressure caused by microspheres injection showed that the microspheres were blocked in the anterior chamber Angle, which increased the resistance of aqueous humor outflow and led to increased intraocular pressure.

OCT and pathological examination showed that the retinal ganglion cells in the rabbit eyes with high intraocular pressure were significantly reduced, the arrangement was disordered, the ganglion vacuoles were seen, the nerve fiber layer was atrophic, the chamber Angle was round and dull, the ciliary blood vessels were filled with red blood cells, and some of them were adherent to the corneal endothelium. The thickness of RNFL and GCIPL became thinner. This provides evidence that the rabbit model of chronic glaucoma was successfully established in this experiment.

At present, the pathogenesis of glaucoma is not fully understood [16], and the discussion of its pathogenesis and the analysis of pathological changes are also the focus of this study. Previous studies mainly focused on the histopathology of the aqueous humor outflow channel, such as tissue plaque accumulation that hinders the outflow channel of aqueous humor or leads to insufficient nutrient supply of trabeculae, degeneration of trabecular meshwork collagen fibers that affect trabecular function, collapse of Schlemm's canal, and narrowing of collecting ducts [17]. In recent years, it has been studied that the activation of glial cells exists in the state of high intraocular pressure [18]. Therefore, in the present study, we used anti-GFAP and anti-GS antibodies as stellate cell markers and Muller cell markers to analyze glial cells. In eyes with normal intraocular pressure, astrocytes are

confined only to the retinal ganglion cell layer. GFAP is expressed in Muller cell processes (gliosis) of eyes with high intraocular pressure. These results suggest that glial cell activation occurs during glaucoma. Muller cell bodies are located in the inner nuclear layer, and Muller cell processes form the inner and outer membrane [19]. The expression of glutamine synthetase (GS) in Muller cells of the ocular hypertension group decreased [20], especially in the ocular hypertension group caused by anterior chamber injection of atropine sulfate microspheres.

In summary, in this study, polymethyl methacrylate (PMMA) microspheres were designed and prepared by polymerization reaction using methyl methacrylate (MMA), hydroxyethyl methacrylate (HEMA) and ethylene glycol dimethacrylate (EDGMA) as raw materials. Hydrogel microspheres have excellent properties such as loose and porous, controllable size, and good biocompatibility, which have broad research prospects as drug delivery tools. The use of PMMA* microspheres as a drug carrier can improve the bioavailability of drugs and achieve efficient release at the retention site of microspheres, which is conducive to the accurate delivery of drugs and the establishment of a more efficient rabbit glaucoma model. This work also provides new ideas for using PMMA* microspheres as drug delivery tools for other applications.

References

[1] Jonas J.B., et al., Glaucoma [J]. The Lancet, 2017. 390(10108): p. 2183-2193.

[2] Ishikawa M., et al., Experimentally Induced Mammalian Models of Glaucoma [J]. Biomed Res Int, 2015. 2015: p. 281214.

[3] Xie M.S., et al., Experimental circumferential canaloplasty with a new Schlemm canal microcatheter [J]. Int J Ophthalmol, 2018. 11(1): p. 1-5.

[4] Scott H. Greenstein, M.D., David H. et al., Systemic Atropine and Glaucoma [J], 1984, Vol. 60, No. 10.

[5] Tawakoli P.N., et al., Comparison of different live/dead stainings for detection and quantification of adherent microorganisms in the initial oral biofilm [J]. Clin Oral Investig, 2013. 17(3): p. 841-50.

[6] Deshpande G., et al., Structural evaluation of preperimetric and perimetric glaucoma. Indian[J]. Ophthalmol, 2019. 67(11): p. 1843-1849.

[7] Clark D.P. and C.T. Badea, Advances in micro-CT imaging of small animals [J]. Phys Med, 2021. 88: p. 175-192.

[8] Gellrich M.M., The slit lamp as videography console: Video article[J]. Ophthalmologe, 2018. 115(10): p. 885-892.

[9] Hu X., et al., Interplay between Muller cells and microglia aggravates retinal inflammatory response in experimental glaucoma. [J]. Neuroinflammation, 2021. 18(1): p. 303.

[10] Mohan N., et al., Newer advances in medical management of glaucoma. Indian [J]. Ophthalmol, 2022. 70(6): p. 1920-1930.

[11] Manuel González de la Rosa, Glaucoma crónico de ángulo abierto [J]. Med Clin (Barc).2005;124(12):461-6.

[12] Kang I.G., et al., Hydroxyapatite Microspheres as an Additive to Enhance Radiopacity, Biocompatibility, and Osteoconductivity of Poly(methyl methacrylate) Bone Cement[J]. Materials (Basel), 2018. 11(2).

[13] van Zyl T., et al., Cell atlas of aqueous humor outflow pathways in eyes of humans and four model species provides insight into glaucoma pathogenesis [J]. Proc Natl Acad Sci U S A, 2020. 117(19): p. 10339-10349.

[14] Pang I.H. and A.F. Clark, Inducible rodent models of glaucoma [J]. Prog Retin Eye Res, 2020. 75: p. 100799.

[15] Yun H, Lathrop KL, Yang E, et al. Angle Closure Glaucoma Precipitated by Aerosolized Atropine.[J].PLoS One, 2014, 9(9): e107446.

[16] Urbonaviciute D., D. Buteikiene and I. Januleviciene, A Review of Neovascular Glaucoma: Etiology, Pathogenesis, Diagnosis, and Treatment. [J]. Medicina (Kaunas), 2022. 58(12).

[17] Jiang S., M. Kametani, D.F. Chen, Adaptive Immunity: New Aspects of Pathogenesis Underlying Neurodegeneration in Glaucoma and Optic Neuropathy. [J]. Front Immunol, 2020. 11: p. 65.

[18] Bell K., et al., Modulation of the Immune System for the Treatment of Glaucoma. [J]. Current Neuropharmacology, 2018. 16(7): p. 942-958.

[19] Auler N., et al., Antibody and Protein Profiles in Glaucoma: Screening of Biomarkers and Identification of Signaling Pathways. [J]. Biology (Basel), 2021. 10(12).

[20] Gionfriddo J.R., et al., Alpha-Luminol prevents decreases in glutamate, glutathione, and glutamine synthetase in the retinas of glaucomatous DBA/2J mice. [J]. Vet Ophthalmol, 2009. 12(5): p. 325-32.